

1 **ASYMPTOMATIC HERPES SIMPLEX VIRUS BRAIN INFECTION ELICITS CELLULAR**  
2 **SENESCENCE PHENOTYPES IN THE CENTRAL NERVOUS SYSTEM OF MICE SUFFERING**  
3 **MULTIPLE SCLEROSIS-LIKE DISEASE**

4

5 **Luisa F. Duarte<sup>1,2</sup>, Verónica Villalobos<sup>1,3</sup>, Mónica A. Farías<sup>1,4</sup>, Ma. Andreina Rangel-Ramírez<sup>1,2</sup>,**  
6 **Enrique González-Madrid<sup>1,2</sup>, Areli J. Navarro<sup>1,4</sup>, Javier Carbone-Schellman<sup>1,4</sup>, Angélica**  
7 **Domínguez<sup>5</sup>, Alejandra Alvarez<sup>1,4</sup>, Claudia A. Riedel<sup>1,2</sup>, Susan M. Bueno<sup>1,4</sup>, Alexis M. Kalergis<sup>1,4,6</sup>,**  
8 **Mónica Cáceres<sup>1,3,\*</sup> and Pablo A. González<sup>1,4,\*</sup>**

9

10 <sup>1</sup>Millennium Institute on Immunology and Immunotherapy, Santiago, Chile.

11 <sup>2</sup>Departamento de Ciencias Biológicas, Facultad de Ciencias de La Vida, Universidad Andrés Bello,  
12 Santiago, Chile.

13 <sup>3</sup>Program of Cellular and Molecular Biology, Institute of Biomedical Sciences, Faculty of Medicine,  
14 Universidad de Chile, Millennium Nucleus of Ion Channel-Associated Diseases (MiNICAD), Santiago,  
15 Chile.

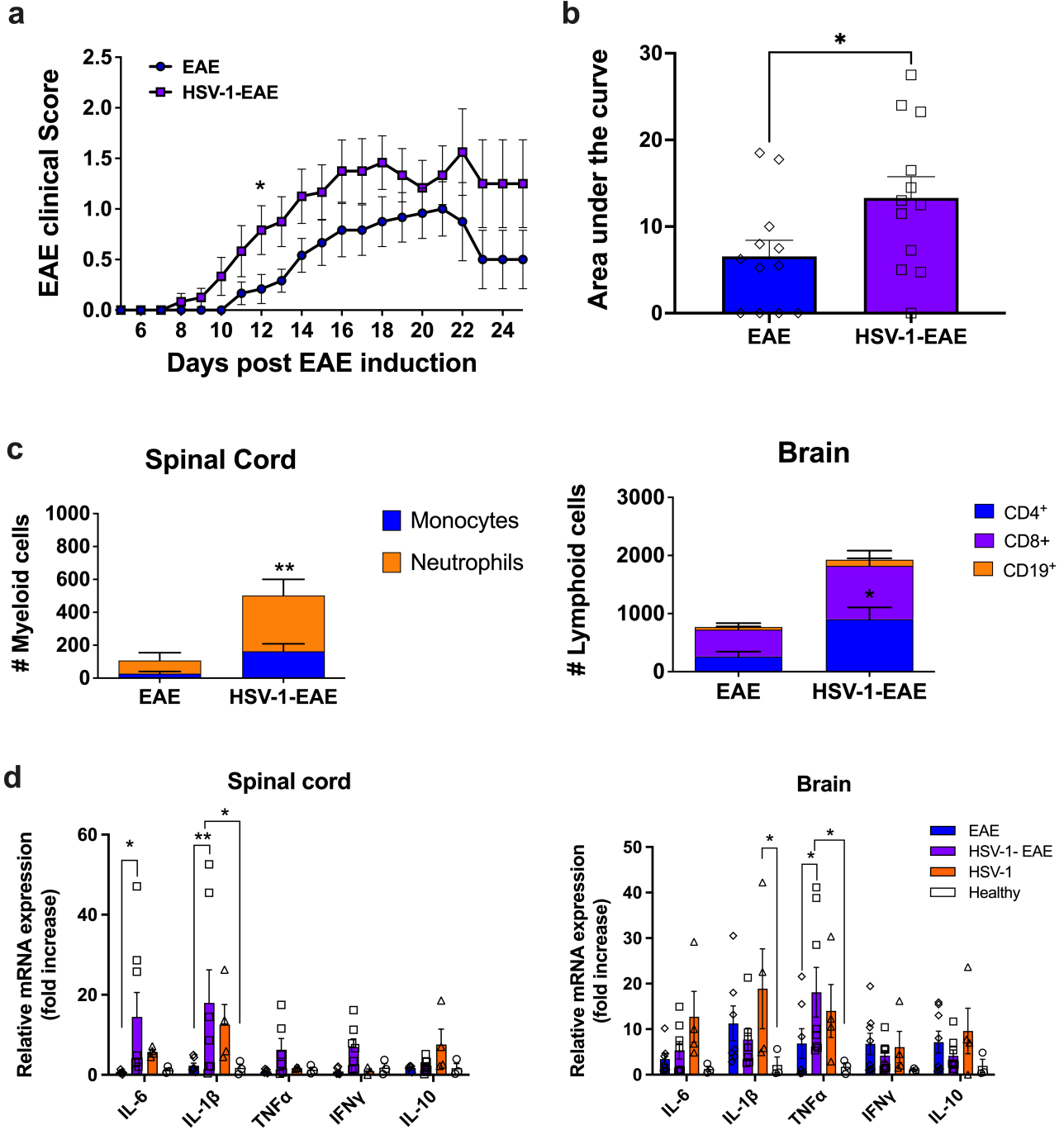
16 <sup>4</sup>Facultad de Ciencias Biológicas, Pontificia Universidad Católica de Chile, Santiago, Chile.

17 <sup>5</sup>Departamento de Salud Pública, Facultad de Medicina, Pontificia Universidad Católica de Chile,  
18 Santiago, Chile.

19 <sup>6</sup>Departamento de Endocrinología, Facultad de Medicina, Pontificia Universidad Católica de Chile,  
20 Santiago, Chile.

21

22 \*Correspondence: Dr. Pablo González, Millennium Institute on Immunology and Immunotherapy,  
23 Facultad de Ciencias Biológicas, Pontificia Universidad Católica de Chile, Av. Portugal 49, Santiago  
24 E-8330025, Chile. E-mail: [pagonzam@uc.cl](mailto:pagonzam@uc.cl) and Dr. Mónica Cáceres, Millennium Institute on  
25 Immunology and Immunotherapy, Instituto de Ciencias Biomédicas, Facultad de Medicina,  
26 Universidad de Chile, Independencia 1027 Santiago, Chile. E-mail: [monicacaceres@med.uchile.cl](mailto:monicacaceres@med.uchile.cl)



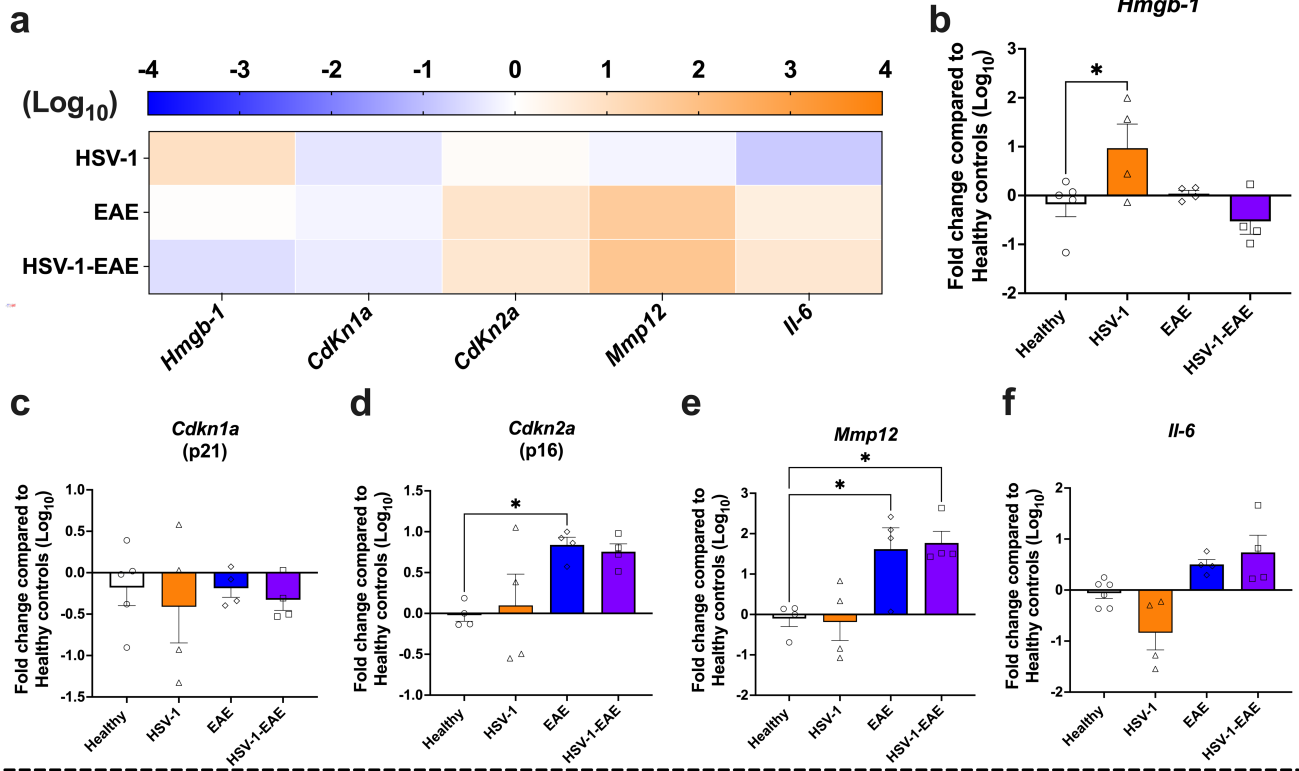
28

29

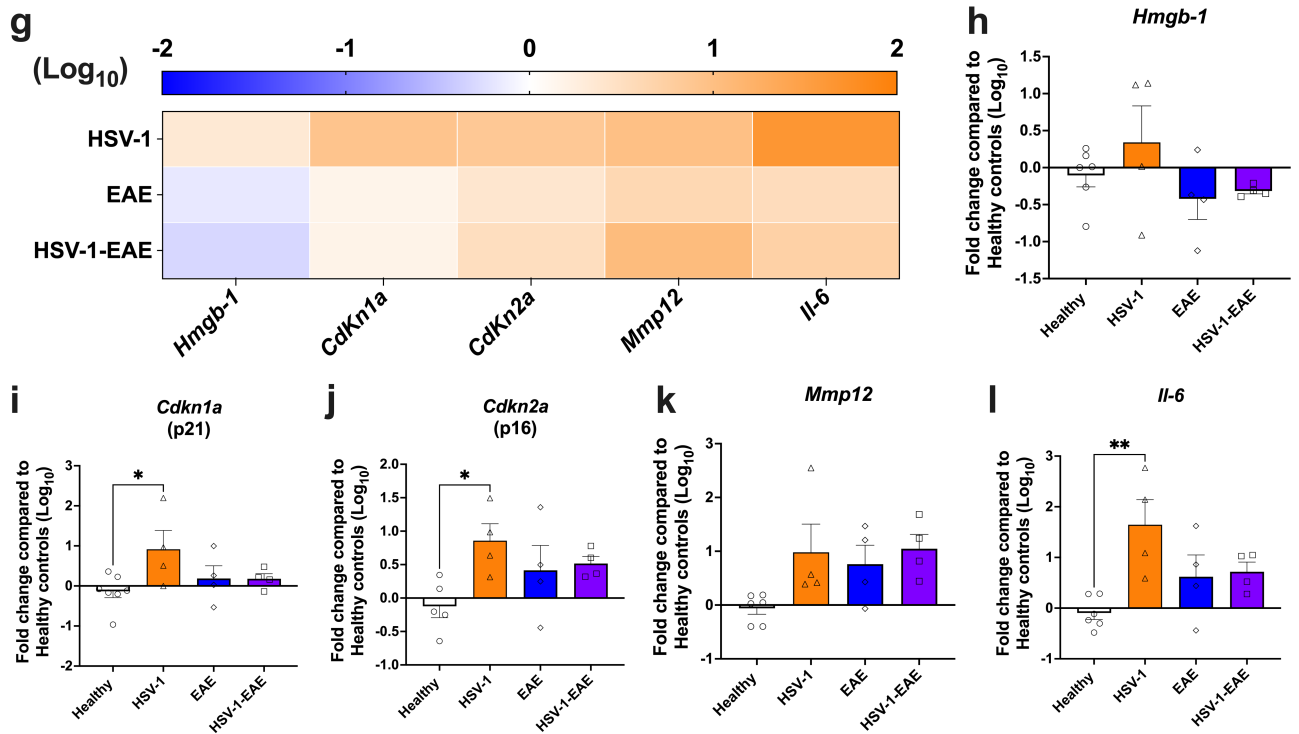
30 **Supplementary figure 1: Asymptomatic HSV-1 Infection causes an earlier onset and more**  
 31 **severe EAE.** **a** EAE clinical score was plotted for 12 mice after EAE induction. EAE was induced 30–  
 32 35 days post-HSV-1 asymptomatic brain infection. The graph shows the means of disease scores  $\pm$

33 SEM for mice mock-treated (blue circles) or infected with WT HSV-1 (17syn<sup>+</sup> strain, purple squares).  
34 The data were analyzed using Multiple Mann-Whitney test, \*p<0.05. **b** The area under the curve (AUC)  
35 integrates the clinical EAE scores and their duration between days 0-25. Data shown are means ±  
36 SEM of three independent experiments. Blue bars with diamonds represent data from mice with EAE  
37 and purple bars with squares represent data from mice with EAE and HSV-1 infection. The data were  
38 analyzed using an unpaired two-tailed Student's t-test, \*p<0.05. **c** Graphs show the whole number of  
39 infiltrating myeloid cells in the spinal cord (left panel) and infiltrating lymphoid cells in the brain (right  
40 panel) of mice induced to develop EAE with or without previous HSV-1 infection. Data are means ±  
41 SEM of two independent experiments n=8 animals/group. The data were analyzed using Two-way  
42 ANOVA followed by Bonferroni's post-test, \*\*p<0.01 \*p<0.05. **d** Relative levels of mRNA of genes  
43 encoding pro-inflammatory cytokines IL-6, IL1-β, TNF-α, and IFN-γ, and the anti-inflammatory  
44 cytokine IL-10 in the spinal cord (left panel) and the brain (right panel) of HSV-1-infected mice with or  
45 without EAE, compared to the mock-EAE group. Blue bars with diamonds represent data from mice  
46 with EAE, purple bars with squares represent data from mice with EAE and HSV-1 infection, orange  
47 bars with triangles represent data from mice with HSV-1 infection without EAE, and white bars with  
48 circles represent data from healthy mice. Values represent means ± SEM of two independent  
49 experiments (n=8 animals/group). Data were analyzed using two-way ANOVA followed by Tukey's  
50 post-test; \*\*p<0.01, and \*p<0.05. The data presented in this figure was previously published in Duarte  
51 *et al.*, 2021 available at doi:10.3389/fimmu.2021.635257. Data from **a-d** were modified from Duarte *et*  
52 *al.*, 2021 to provide a summary and more focused information for this study. Permission to use these  
53 figures is granted by CC-BY Creative Commons attribution license used by the publisher.

## SPINAL CORD



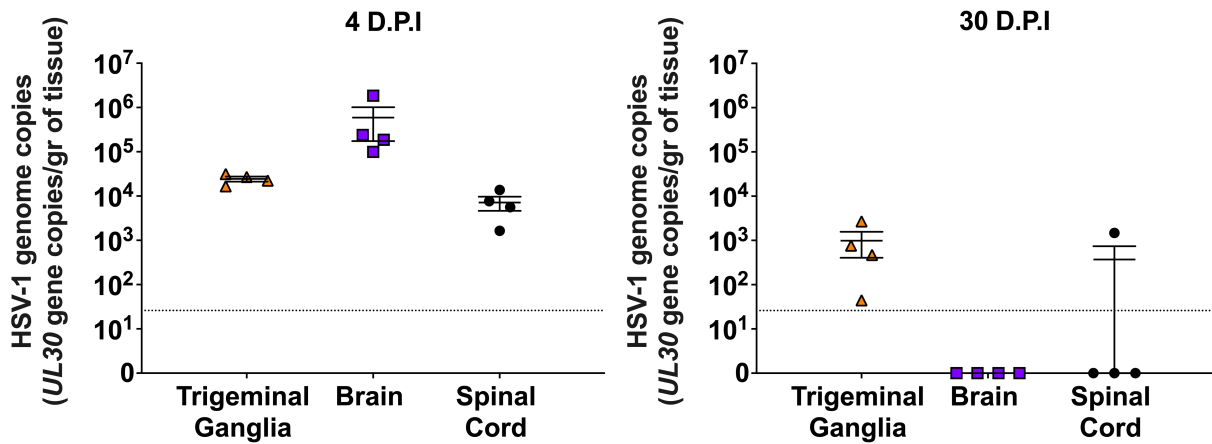
## BRAIN



55 **Supplementary figure 2: mRNA levels of senescence-associated genes in the CNS increase 21**  
56 **days after EAE induction regardless of prior HSV-1 infection.** Mice were mock-treated (healthy  
57 group, white bars with circles) or asymptotically infected with HSV-1 strain 17syn<sup>+</sup> in the brain  
58 (HSV-1 group, orange bars with triangles). EAE was induced four weeks after mock treatment (EAE  
59 group, blue bars with diamonds), or HSV-1 infection (HSV-1-EAE group, purple bars with squares).  
60 Spinal cord and brain homogenates were recovered 21 days after EAE induction (EAE and HSV-1-  
61 EAE groups) or 52 days after HSV-infection (HSV-1 group). The expression of senescence-associated  
62 genes was evaluated at the mRNA level by RT-qPCR by using the  $2^{-\Delta\Delta CT}$  method with *Actb* as a  
63 reference gene ( $\beta$ -actin protein). **a** Heatmap comparing mRNA levels of senescence-associated  
64 genes in the spinal cord. Orange color indicates upregulation, while blue color indicates  
65 downregulation. Stronger colors indicate stronger effects. Relative mRNA expression of the gene  
66 products **b** *Hmgb-1*, **c** *Cdkn1a*, **d** *Cdkn2a*, **e** *Mmp12*, and **f** *Il6* in the spinal cord homogenates of the  
67 different mouse groups compared to healthy controls. **g** Heatmap comparing mRNA levels of  
68 senescence-associated genes in the brain. Orange color indicates upregulation, while blue color  
69 indicates downregulation. Stronger colors indicate stronger effects. Relative mRNA expression of the  
70 gene products **h** *Hmgb-1*, **i** *Cdkn1a*, **j** *Cdkn2a*, **k** *Mmp12*, and **l** *Il6* in the brain homogenates of the  
71 different mouse groups compared to healthy controls. Values represent means  $\pm$  SEM of 4  
72 animals/group. Log-transformed data were analyzed using One-way ANOVA followed by Dunnett's  
73 post-test; \*\*p<0.01, and \*p<0.05.

74

75



76

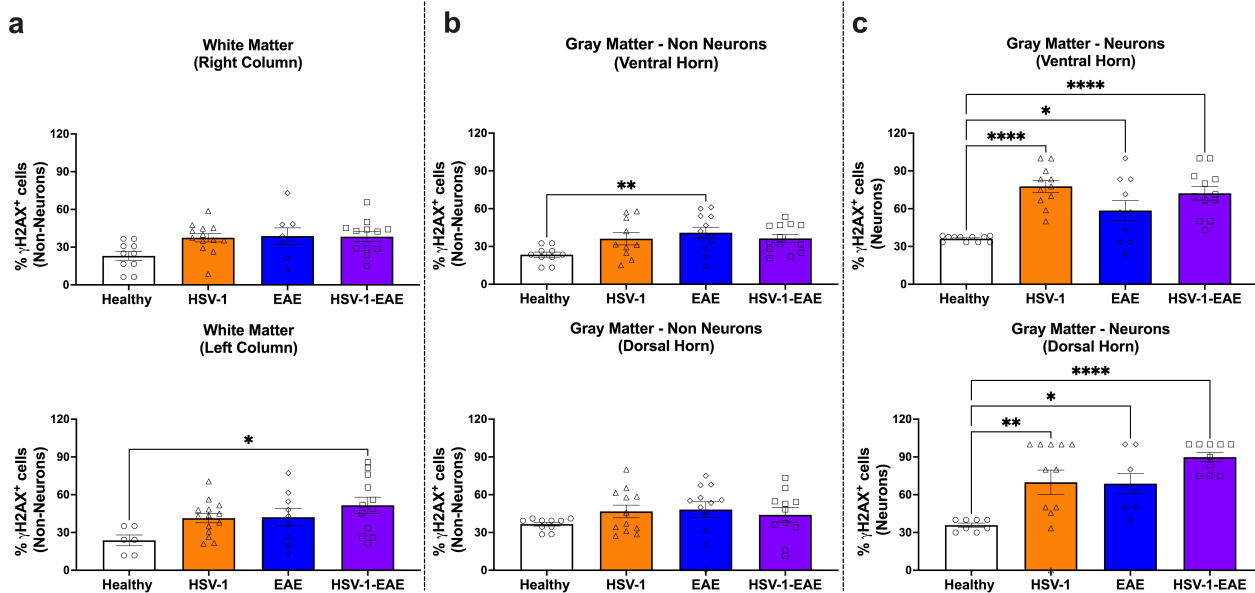
77

78 **Supplementary figure 3: Viral loads in the nervous system after sublethal asymptomatic**  
 79 **infection with HSV-1 by intranasal route.** C57BL/6 mice were intranasally mock-treated or infected  
 80 with HSV-1 (17syn+ strain) and followed for 30 days. HSV-1 *UL30* gene copies per gram of trigeminal  
 81 ganglia (orange triangles), brain (purple squares) and spinal cord (black circles) was determined at 4-  
 82 and 30-days post-infection by qPCR (values normalized to uninfected mice, n=4 animals/group). Data  
 83 were analyzed using One-way ANOVA followed by Dunnett's post-test. There were no statistically  
 84 significant differences between groups. Dashed lines indicate the limit of detection of viral genome  
 85 copies (>26 viral genome copies per 200 ng of extracted DNA) based on samples obtained from each  
 86 type of tissue from the mock-treated group.

87

88

89



90

91 **Supplementary figure 4: DNA damage-related foci are observed in neurons and non-neurons**

92 **cells 21 days after EAE induction in the spinal cord tissues.** Spinal cord tissue was harvested 21

93 days after EAE induction (EAE and HSV-1-EAE groups) and 52 days after HSV-1 infection (HSV-1

94 group) for detecting the phosphorylation of histone H2AX (γH2AX) by immunohistochemistry. **a**

95 Quantification of γH2AX foci in the nucleus of non-neuron cells in the white matter (analysis separated

96 in right and left columns, upper and lower panels, respectively). **b** Quantification of γH2AX foci in the

97 nucleus of non-neuron cells in the gray matter (analysis separated in ventral and dorsal horns, upper

98 and lower panels, respectively). **c** Quantification of γH2AX foci in the nucleus of neuron cells in the

99 gray matter (analysis separated in ventral and dorsal horns upper and lower panels, respectively).

100 Values represent means ± SEM of the percentage of γH2AX-positive cells of four mice per group.

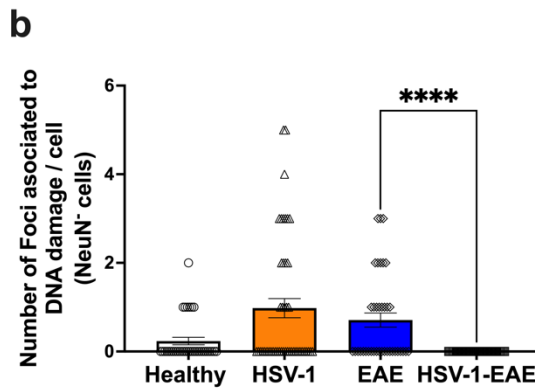
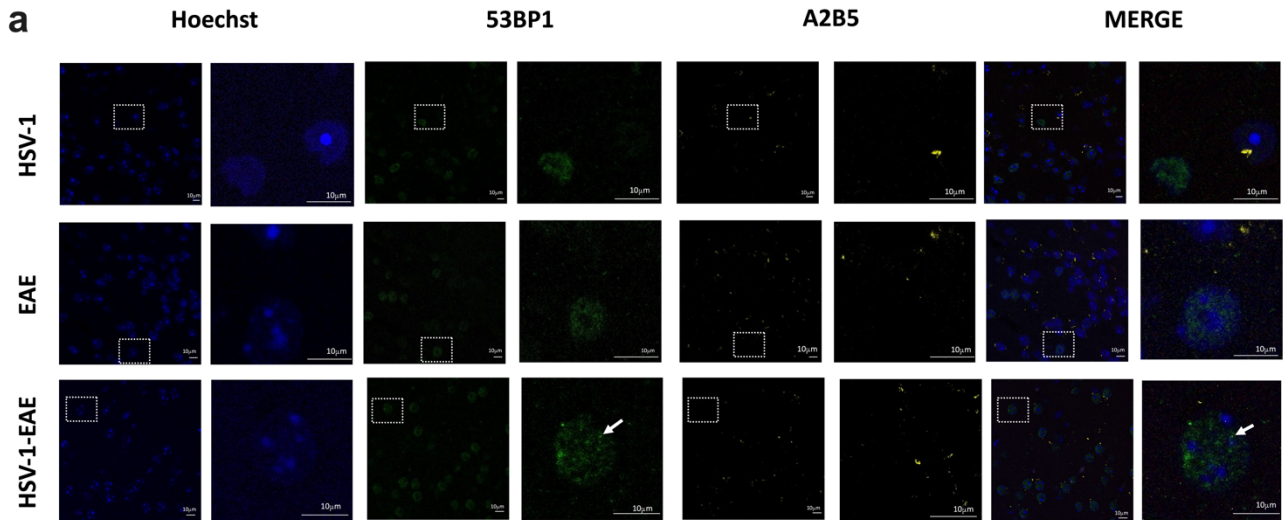
101 Data were analyzed using One-way ANOVA followed by Bonferroni's post-test; \*\*\*\*p<0.001, \*\*p<0.01,

102 \*p<0.05. White bars with circles represent data from healthy mice, orange bars with triangles represent

103 data from mice with HSV-1 infection, blue bars with diamonds represent data from mice with EAE and

104 purple bars with squares represent data from mice with EAE and HSV-1 infection.

105



106

107

108

109

110

111

112

113

114

115

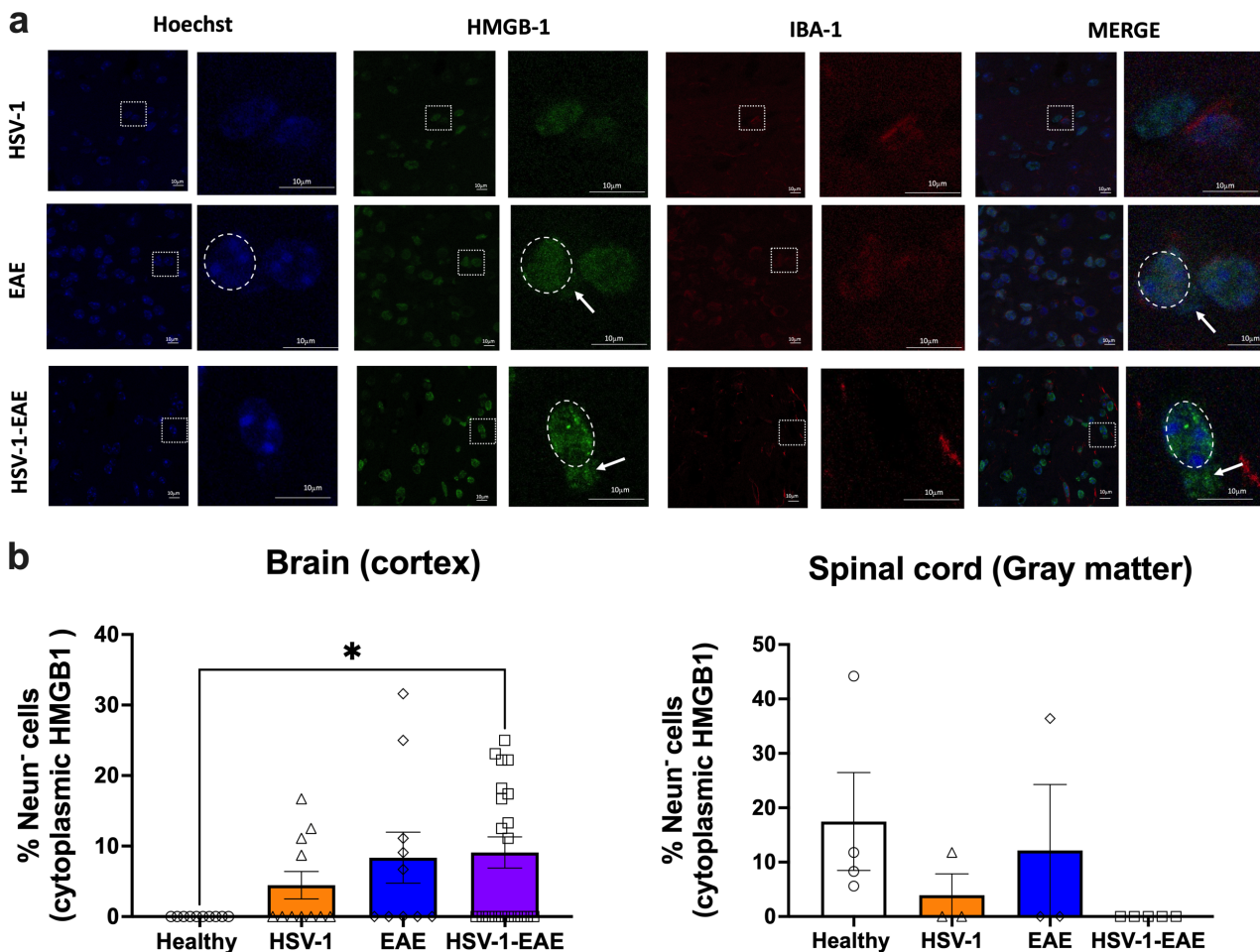
116

117

**Supplementary figure 5: DNA damage-related foci are rare or absent in non-neuronal cells within the brain of mice with asymptomatic HSV-1 brain infection and/or EAE.** Brain tissues were harvested 14 days after EAE induction or 45 days after asymptomatic HSV-1 brain infection, or mock treatment alone for detecting the 53BP1 protein which is used as a DNA damage marker by immunofluorescence. **a** Representative images showing Hoechst nuclei staining (blue color), 53BP1 staining (green color), A2B5 staining (yellow color, oligodendrocyte progenitor marker), and image merges. Left: images for each fluorescence channel correspond to 100X magnifications and right: images are shown at a 5X optic zoom of the area outlined in squares with white dashed lines. Scale bars = 10  $\mu$ m. White arrows show accumulation of 53BP1 into DNA damage foci. **b** Quantification of foci associated to DNA Damage in the nucleus of NeuN<sup>+</sup> cells. Values represent means  $\pm$  SEM of the measurements carried out in at least ten fields per sample. Data were analyzed using Kruskal-Wallis



118 followed by Dunn's post-test; \*\*\*\* $p < 0.001$ . White bars with circles represent data from healthy mice,  
 119 orange bars with triangles represent data from mice with HSV-1 infection, blue bars with diamonds  
 120 represent data from mice with EAE and purple bars with squares represent data from mice with EAE  
 121 and HSV-1 infection.  
 122  
 123



124

125 **Supplementary figure 6: The release of HMGB-1 from the nucleus to the cytoplasm is observed**  
 126 **in non-neuronal cells in the brains of mice experiencing HSV-1 brain infection and/or EAE.**

127 Brain and spinal cord tissues were harvested 14 days after EAE induction, 45 days after HSV-1  
 128 infection, or from mock-treated mice for detecting the expression and release of HMGB-1 by  
 129 immunofluorescence. **a** Representative images showing Hoechst nuclei staining (blue color), HMGB-

130 1 staining (green color), IBA-1 staining (red color, an activated microglia marker), and image merges.

131 Left: images for each fluorescence channel correspond to 100X magnifications and right: images are

132 shown at a 5X optic zoom of the area outlined in squares with white dashed lines. Scale bars = 10

133  $\mu\text{m}$ . White arrows show the translocation of HMGB-1 from the nucleus to the cytoplasm. **b** Graphs

134 show the percentage of NeuN<sup>+</sup> cells with HMBG-1 release from the nucleus toward cytoplasm in the

135 brain cortex (left) and in the gray matter of the spinal cord (right). Values represent means  $\pm$  SEM of

136 the measurements carried out in at least ten fields in the brain tissues and three fields in the spinal

137 cord tissues per sample. Data were analyzed using Kruskal-Wallis followed by Dunn's post-test;

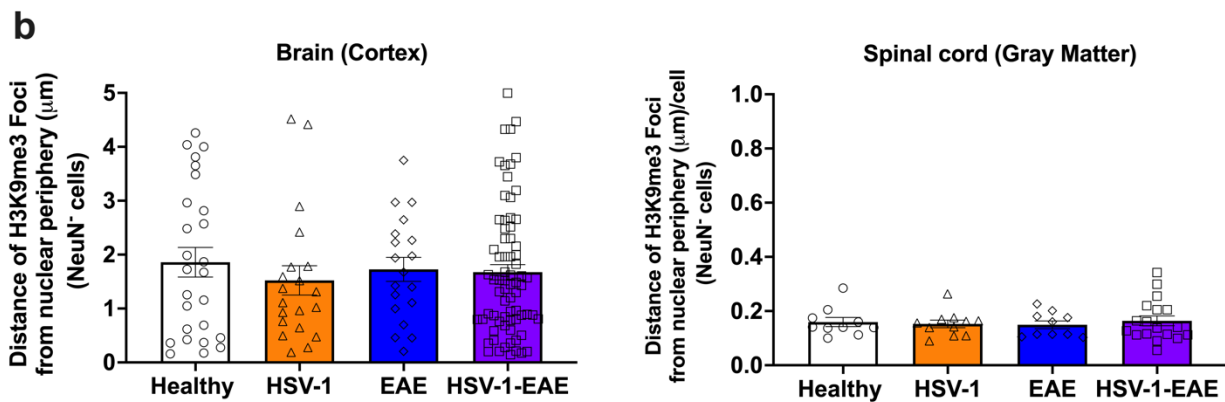
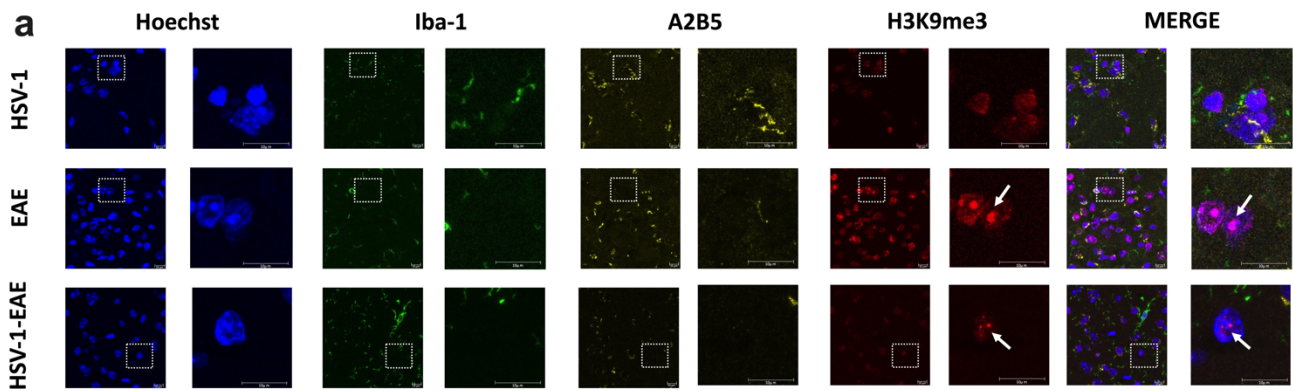
138 \* $p < 0.05$ . White bars with circles represent data from healthy mice, orange bars with triangles represent

139 data from mice with HSV-1 infection, blue bars with diamonds represent data from mice with EAE and

140 purple bars with squares represent data from mice with EAE and HSV-1 infection.

141

142



143

144 **Supplementary figure 7: H3K9me3-associated foci are sparse in non-neuron cells in the brain**  
145 **and spinal cord tissues of mice with asymptomatic HSV-1 brain infection and/or EAE.** Brain and  
146 spinal cord tissues were harvested 14 days after EAE induction, and 45 days after HSV-1 infection,  
147 or from mock-treated mice for detecting the expression of H3K9me3 foci by immunofluorescence. **a**  
148 Representative images showing Hoechst nuclei staining (blue color), IBA-1 staining (green color,  
149 microglia marker), A2B5 staining (yellow color, an oligodendrocyte progenitor marker), H3K9me3  
150 staining (red color), and image merges. Left: images in each fluorescence channel correspond to 100X  
151 magnifications, and right: Images are shown at a 5X optic zoom of the area outlined in squares with  
152 white dashed lines. Scale bars = 10  $\mu$ m. White arrows show senescence-associated heterochromatin  
153 foci (SAHF). **b** Quantification of the distance of each H3K9me3 foci from the nuclear periphery in  
154 NeuN-negative cells. Values represent means  $\pm$  SEM of the measurements carried out in at least ten  
155 fields in the brain tissues and three fields in the spinal cord tissues per sample. Data were analyzed  
156 using Kruskal-Wallis followed by Dunn's post-test. There were no statistically significant differences  
157 between groups. White bars with circles represent data from healthy mice, orange bars with triangles  
158 represent data from mice with HSV-1 infection, blue bars with diamonds represent data from mice  
159 with EAE and purple bars with squares represent data from mice with EAE and HSV-1 infection.